

# Third-harmonic generation with cylindrical Gaussian beams

Dan Oron and Yaron Silberberg

*Department of Physics of Complex Systems, The Weizmann Institute of Science, Rehovot 76100, Israel*

Received December 1, 2003; revised manuscript received March 23, 2004; accepted June 16, 2004

Performing third-harmonic-generation (THG) microscopy with a cylindrically focused Gaussian beam results in significant differences from standard THG microscopy owing to the different phase-matching geometry. These differences are characterized analytically in the slowly varying envelope approximation. It is shown that THG is not observed in samples with normal dispersion even for line illumination. We use this to perform video-rate THG microscopy. © 2004 Optical Society of America

OCIS codes: 110.6880, 180.5810, 190.4160, 190.7110.

## 1. INTRODUCTION

The application of nonlinear optical processes, such as harmonic generation, has been rapidly developing since the appearance of compact femtosecond lasers. In particular, third-harmonic generation (THG), which has traditionally been used for characterization of the nonlinear polarizability of substances, has found a new application in coherent multiphoton microscopy.

In multiphoton microscopy a nonlinear process is excited at the focal point of a tightly focused laser beam. Measuring this nonlinear signal results in intrinsic depth resolution and an improved signal-to-background ratio compared with standard microscopic techniques. The first multiphoton microscopy experiments applied two-photon<sup>1</sup> and three-photon<sup>2</sup> fluorescence, both incoherent processes, for imaging. Coherent multiphoton techniques such as second-harmonic generation,<sup>3</sup> THG,<sup>4–8</sup> and coherent anti-Stokes Raman spectroscopy<sup>9–12</sup> have recently become attractive alternatives for depth-resolved imaging of unstained samples.

Like all laser-scanning microscopy methods, multiphoton microscopy techniques suffer from relatively long image-acquisition times. Owing to the relatively weak nonlinear signal, integration times of the order of 1 ms/pixel are typically used. Serial acquisition of a reasonably sized image thus takes several seconds. Two methods have recently been developed to significantly reduce the image-acquisition time while maintaining the depth resolution. Both methods are based on illumination of more than one pixel at a time and the use of an imaging detection system. The simpler method uses line illumination; i.e., the illuminating beam is tightly focused along one transverse axis and weakly focused along the other.<sup>13</sup> Scanning is thus performed only along one spatial direction. This method results in a somewhat reduced depth resolution and has been applied only to two-photon excitation fluorescence. The second method involves the use of a microlens array<sup>14–17</sup> or a diffractive optical element,<sup>18</sup> essentially splitting the illuminating beam into an array of beams, each producing a nearly diffraction-limited spatially separated spot within the sample. Using this

method, one performs imaging either by scanning a significantly smaller area in both spatial directions or by rotating the microlens array.<sup>16</sup> The rotating microlens array method has recently been used also for obtaining video-rate second-harmonic-generation images.<sup>19</sup>

Here we consider the use of line illumination in THG. Since THG is a coherent process, and unlike the case of multiphoton fluorescence,<sup>13</sup> the illumination geometry has a significant effect on the generated signal owing to phase-matching considerations.<sup>20</sup> We first approach this by presenting an analytic solution of the problem of THG by using two-dimensional (2D) focused Gaussian beams. This is then compared with the well-known three-dimensional (3D) solution.<sup>21</sup> As it turns out, for most practical purposes, line illumination can still be used for THG imaging. Some conditions exist, however, under which subtle differences exist between the two cases. We discuss the origin of this phenomenon and possible applications. Finally, we demonstrate the use of line illumination for video-rate THG microscopy.

## 2. MATHEMATICAL FORMULATION OF THIRD-HARMONIC GENERATION WITH TWO-DIMENSIONAL FOCUSED GAUSSIAN BEAMS

In analogy with the case of a 3D focused Gaussian beam,<sup>21</sup> we get for a freely propagating 2D focused Gaussian beam a solution of the form

$$A(x, z) = \frac{A_1}{\sqrt{1 + i\zeta}} \exp\left[-\frac{x^2}{w_0^2(1 + i\zeta)}\right], \quad (1)$$

where  $\zeta = 2z/b$  is the dimensionless longitudinal coordinate defined in terms of the confocal parameter  $b = kw_0^2$  and  $w_0$  is the beam waist. This solution is closely related to that of a 3D beam,<sup>21</sup>

$$A(x, y, z) = \frac{A_1}{1 + i\zeta} \exp\left[-\frac{x^2 + y^2}{w_0^2(1 + i\zeta)}\right], \quad (2)$$

but diverges more slowly in the longitudinal direction. The resulting  $q$ th harmonic can be derived by assuming an undepleted pump and taking the nonlinear polarization as  $\chi^{(q)}A_1^q$ . From this we get

$$2ik_q \frac{\partial A_q}{\partial z} + \frac{\partial^2 A_q}{\partial x^2} = -\frac{4\pi(q\omega)^2}{c^2} \chi^{(q)}A_1^q \exp(i\Delta kz), \quad (3)$$

with the phase mismatch  $\Delta k = qk_1 - k_3$ . The solution to this equation is also a 2D Gaussian beam of the form

$$A_q(x, z) = \frac{A_q(z)}{\sqrt{1+i\zeta}} \exp\left[-\frac{qx^2}{w_0^2(1+i\zeta)}\right], \quad (4)$$

which has to fulfill

$$\frac{dA_q}{dz} = \frac{i2q\pi\omega}{nc} \chi^{(q)}A_1^q \frac{\exp(i\Delta kz)}{(1+i\zeta)^{(q-1)/2}}. \quad (5)$$

This solution is, again, slightly different from that obtained for 3D Gaussian beams, where the exponent of  $(1+i\zeta)$  is replaced by  $q-1$ . This, again, reflects the slower divergence of the beam in the 2D case.

This difference alters the dependence of the total THG intensity from an infinite bulk medium on the phase mismatch. Asymptotically, the 2D solution is of the form

$$I_{2D} \propto \begin{cases} 0, & \Delta k < 0 \\ \frac{1}{2}, & \Delta k = 0, \\ \exp(-b\Delta k), & \Delta k > 0 \end{cases} \quad (6)$$

whereas in the 3D case

$$I_{3D} \propto \begin{cases} 0, & \Delta k \leq 0 \\ (b\Delta k)^2 \exp(-b\Delta k), & \Delta k > 0 \end{cases} \quad (7)$$

These two asymptotes are shown as gray curves in Fig. 1. In both cases a positive phase mismatch is necessary to compensate for the Gouy phase shift experienced at the focus.<sup>20</sup> In the figure we also show the normalized THG intensity, as calculated by numerical integration of Eq. (5), from a bulk sample with a thickness of ten confocal parameters, assuming the fundamental beam is focused at its center. As can be seen, the 3D solution is almost indistinguishable from the limit of an infinitely thick medium, and the THG signal practically vanishes not only for normal dispersion but even in the case of perfect phase matching.

The behavior in the 2D case is somewhat different. An oscillatory behavior, especially dominant for small positive phase mismatch, is observed for a finite sample. This is due to contributions to the total THG signal from the edges of the sample, and the oscillation period is thus determined by the sample thickness. Since in two dimensions the beam diverges much more slowly, these oscillatory contributions are not negligible.

Looking at the two curves for both the 2D and the 3D cases, one can distinguish three regions. For negative phase mismatch (normal dispersion), the THG signal practically vanishes for both 2D and 3D beams. Since this is the region in which most THG microscopy experiments are conducted, such experiments can be conducted

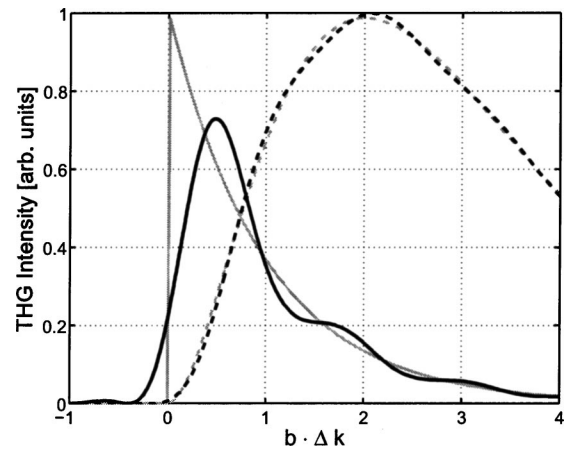


Fig. 1. Normalized THG signal, derived by integrating Eq. (5), as a function of the nondimensional phase mismatch  $b\Delta k$  for a Gaussian beam focused within a finite medium (depth of  $10b$ ) for the cases of a 2D focused Gaussian beam (solid black curve) and a 3D focused Gaussian beam (dashed black curve). Also plotted are the corresponding asymptotic values for an infinite medium (gray curves). As can be seen, the medium is sufficiently thick only for the 3D result to reach its asymptotic value.

also with line illumination without changing the most dominant feature of THG imaging, i.e., the absence of signal from bulk homogeneous samples. For perfect phase matching or a very small nondimensional positive phase mismatch, the THG signal from a 2D beam can significantly exceed that from a 3D beam. This region can be of interest either in the gas phase, in which the phase mismatch is exceedingly small, or when the samples exhibit birefringence.<sup>22–24</sup> For large values of the nondimensional phase mismatch, the THG from a 3D beam is significantly stronger than that from a 2D one.

### 3. THIRD-HARMONIC-GENERATION MICROSCOPY WITH A CYLINDRICAL BEAM

In practice, THG microscopy is usually performed in media with normal dispersion. Even assuming the tightest focusing and moderate dispersion,  $b\Delta k < -0.2$ . As has been discussed in Section 2, for such values the THG signal practically vanishes not only in the 3D case but also in the 2D one even for finite-sized samples. Thus, even with the use of line scanning in THG microscopy, a signal would not appear from bulk homogeneous regions. In both cases the resulting image highlights only material interfaces and small inclusions.

The most important difference between THG with point illumination and THG with line illumination (or, for that matter, an array of focal points, such as the ones used in Refs. 14–17) is the need for an imaging setup for detection. By use of point illumination, both the depth resolution and the axial resolution are determined by the illumination beam's focal spot. In an imaging setup, the axial resolution is determined by the collection lens. An important outcome of this for coherent processes (such as THG) is that when the illumination spot is larger than the spatial resolution of the collection lens the image of the illumination spot is coherently generated. This may lead to coherent artifacts from features that are unresolved by the collection optics. Thus, to obtain high-

quality images, one must use a high numerical-aperture (NA) collection lens. The observed field of view in an imaging setup can be limited either by the illumination area or by the field of view of the collection lens.

In the following we demonstrate THG imaging with line illumination and discuss the effect of such illumination on the depth resolution.

### A. Experimental System

The laser source used in the experiments is an optical parametric oscillator delivering 130-fs pulses at  $1.5\ \mu\text{m}$  with an energy of approximately 2 nJ at a repetition rate of 80 MHz (Spectra-Physics Opal). For THG microscopy experiments we used a simple homebuilt confocal microscope. Laser light was focused into the sample by use of a NA = 0.85 objective lens. THG light was collected by either a NA = 0.63 objective or a similar NA = 0.85 lens (in the imaging experiment), filtered by a bandpass filter at 500 nm, and measured either by a photomultiplier tube and a lock-in amplifier or by an intensified CCD (in the imaging experiment). For line illumination we added a cylindrical lens in the vertical direction with a focal length of 20 or 25 cm before the entrance to the objective lens. The focal length of this lens determines the aspect ratio of the illumination line. The distance between the two was chosen so that the focal length of the entire system in both transverse directions is the same. Scanning is performed with a galvanometric scanner and a cylindrical X1 magnification telescope in the horizontal direction (built with  $f = 10\text{-cm}$  lenses). The beam is scanned at approximately 250 Hz, so that each frame on the CCD averages over several scans. A schematic setup of the experimental system appears in Fig. 2.

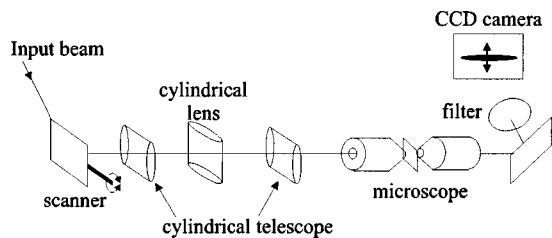


Fig. 2. Schematic setup for THG microscopy experiments with line illumination.

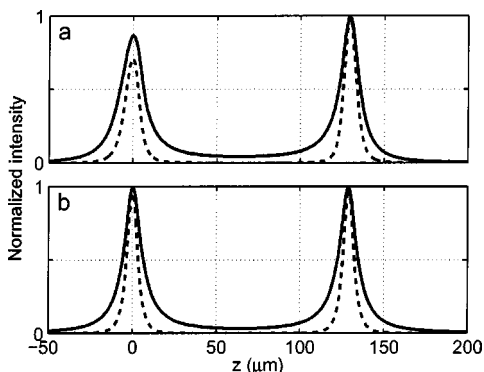


Fig. 3. THG signal in a Z-scan measurement through a  $130\text{-}\mu\text{m}$  cover glass. (a) Measured signal with line illumination (solid curve) and with point illumination (dashed curve). (b) Theoretical prediction for (a) obtained by integrating Eq. (5).

### B. Depth Resolution with a Cylindrical Beam

As has been noted for the case of two-photon excitation fluorescence,<sup>13</sup> the depth resolution for line illumination is worse than for point illumination. This reflects the slower divergence of the beam. The effect of line illumination on the depth resolution is, however, different in the case of THG, again owing to phase-matching considerations. Figure 3a shows the observed THG intensity in a Z-scan measurement through a  $130\text{-}\mu\text{m}$  cover glass. Figure 3b shows the theoretical results as obtained by numerical integration of Eq. (5) with a confocal parameter  $b = 8\ \mu\text{m}$ . In both images the solid curve is obtained with line illumination, and the dashed curve is obtained with point illumination. As can be seen, the agreement with the theoretical prediction is excellent. Differences observed are probably due to aberrations at the entrance facet of the cover glass (since the objective is designed to work with a cover glass). The two air-glass interfaces are clearly observed both for line illumination and for point illumination. The FWHM of the peaks is larger in the case of line illumination by a factor of approximately 1.7. The more dominant effect in the case of line illumination is the slower decay of the signal away from the peak. Thus, despite a FWHM of approximately  $12\ \mu\text{m}$ , the measured THG intensity at the center of the glass cover glass,  $65\ \mu\text{m}$  away from both interfaces, is not zero. Still, the depth resolution is sufficient to perform THG microscopy.

### C. Video-Rate Third-Harmonic-Generation Imaging with a Cylindrical Beam

To demonstrate video-rate THG microscopy, we consider a sample consisting of individual sea urchin larval spicules spread on a glass microscope slide and immersed in an  $n = 1.61$  index-matching oil. By x-ray diffraction measurements the larval spicule has been shown to be made of a single calcite crystal.<sup>25</sup> A more detailed description of THG from larval spicules can be found in Oron *et al.*<sup>23,24</sup> In performing line-scanning THG imaging, there is a trade-off between the necessary frame-acquisition time (or the signal intensity) and the scanned area (determined by the focusing strength of the cylindrical lens). In the following we optimized the imaged area to an acquisition rate of several frames per second.

A THG image of a single triradiate larval spicule, obtained by grabbing a frame from the intensified CCD detector, is shown in Fig. 4. The spicule has three arms at angles of  $120^\circ$  with one another, originating from a central calcite crystal. Each arm is  $1\text{--}2\ \mu\text{m}$  thick and as much as several tens of micrometers long. As can be seen, some background is generated over the entire frame, on top of which a stronger signal is observed from the spicule. The background is due to THG from the glass-immersion oil interface. The weak ringing pattern along the bottom arm of the spicule is a coherent artifact due to the small feature size, which is not fully resolved by the collecting lens. This results, for each illuminated line (i.e., in the horizontal direction) in an interference pattern between the smooth THG generated by the glass-immersion oil interface and the sinc function of the not-fully-resolvable spicule.

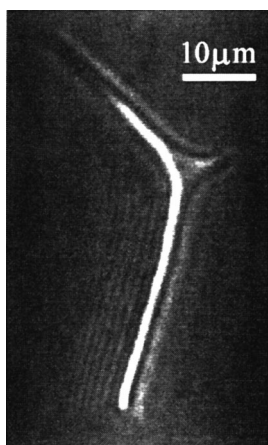


Fig. 4. THG image of a single sea urchin larval spicule spread on a glass slide as obtained by grabbing a frame from the intensified CCD.

#### 4. CONCLUSION

When implementing a space-multiplexed method for fast scanning in coherent multiphoton microscopy, one must take care to consider the effect also on the phase-matching conditions. This is particularly important in THG microscopy, whose most dominant property—the ability to highlight interfaces and small inclusions—is a phase-matching effect.

For most samples (exhibiting normal dispersion) the fundamental property of THG, i.e., the absence of signal from a bulk homogeneous medium, is maintained with line illumination. This enables one to perform video-rate THG microscopy by scanning only a single axis, as has been previously done for two-photon excitation fluorescence.<sup>13</sup> The area that can be covered by the line scanning is dependent on the total energy of the input pulse. In our experiments we used an optical parametric oscillator source at 1500 nm, delivering 2-nJ, 130-fs pulses. This allowed us to illuminate a line with an aspect ratio of approximately 40. Other sources that deliver higher energy and significantly shorter pulses at 1500 nm, such as Cr:YAG lasers, are currently available.<sup>26</sup> Moreover, current Ti:sapphire sources are highly suitable for THG microscopy<sup>27</sup> and can deliver pulses with an energy larger by an order of magnitude. Either of these should allow significantly larger aspect ratios, allowing real-time imaging of large areas.

The theoretical analysis provided here shows, nevertheless, that under some conditions line illumination can have a significant effect on phase-matching conditions. The THG generated with line illumination is significantly larger than that obtained with point illumination in a range of values of the phase mismatch around  $\Delta k = 0$ . In particular, a finite signal is generated for perfect phase matching. This could, for example, be used for THG spectroscopy in the gas phase. It can also be used for polarization THG microscopy,<sup>23</sup> in which the birefringence compensates for material dispersion, in weakly birefringent media.

#### ACKNOWLEDGMENTS

The authors thank N. Dudovich, D. Mandelik, and E. Tal for helpful discussions. Financial support from the Is-

rael Science Foundation and the German Bundesministerium für Bildung, Forschung, und Technologie is gratefully acknowledged.

D. Oron, the corresponding author, can be reached by e-mail at dan.oron@weizmann.ac.il.

#### REFERENCES

1. W. Denk, J. H. Stricker, and W. W. Webb, "Two-photon laser scanning fluorescence microscopy," *Science* **248**, 73–76 (1990).
2. S. Maiti, J. B. Shear, R. M. Williams, W. R. Zipfel, and W. W. Webb, "Measuring serotonin distribution in live cells with three-photon excitation," *Science* **275**, 530–532 (1997).
3. G. Peleg, A. Lewis, O. Bouevitch, L. Loew, D. Parnas, and M. Linal, "Gigantic optical non-linearities from nanoparticle-enhanced molecular probes with potential for selectively imaging the structure and physiology of nanometric regions in cellular systems," *Bioimaging* **4**, 215–224 (1996).
4. Y. Barad, H. Eisenberg, M. Horowitz, and Y. Silberberg, "Nonlinear scanning laser microscopy by third harmonic generation," *Appl. Phys. Lett.* **70**, 922–924 (1997).
5. M. Muller, J. Squier, K. R. Wilson, and G. J. Brakenhoff, "3D-microscopy of transparent objects using third-harmonic generation," *J. Microsc.* **191**, 266–274 (1998).
6. J. A. Squier, M. Muller, G. J. Brakenhoff, and K. R. Wilson, "Third harmonic generation microscopy," *Opt. Express* **3**, 315–324 (1998), <http://www.opticsexpress.org>.
7. D. Yelin and Y. Silberberg, "Laser scanning third-harmonic-generation microscopy in biology," *Opt. Express* **5**, 169–175 (1999), <http://www.opticsexpress.org>.
8. D. Yelin and Y. Silberberg, "Third-harmonic microscopy in biology," *Microsc. Anal.*, Nov. 2000, pp. 13–16.
9. A. Zumbusch, G. R. Holtom, and X. S. Xie, "Three-dimensional vibrational imaging by coherent anti-Stokes Raman scattering," *Phys. Rev. Lett.* **82**, 4142–4145 (1999).
10. J. Cheng, Y. K. Jia, G. Zheng, and X. S. Xie, "Laser-scanning coherent anti-Stokes Raman scattering microscopy and applications to cell biology," *Biophys. J.* **83**, 502–509 (2002).
11. E. O. Potma, W. P. de Boeij, P. J. M. van Haastert, and D. A. Wiersma, "Real-time visualization of intracellular hydrodynamics in single living cells," *Proc. Natl. Acad. Sci. U.S.A.* **98**, 1577–1582 (2001).
12. N. Dudovich, D. Oron, and Y. Silberberg, "Single-pulse coherently controlled nonlinear Raman spectroscopy and microscopy," *Nature* **418**, 512–514 (2002).
13. G. J. Brakenhoff, J. Squier, T. Norris, A. C. Bliton, M. H. Wade, and B. Athey, "Real-time two-photon confocal microscopy using a femtosecond, amplified Ti:sapphire system," *J. Microsc.* **181**, 253–259 (1996).
14. A. H. Buist, M. Muller, J. Squier, and G. J. Brakenhoff, "Real-time two-photon absorption microscopy using multipoint excitation," *J. Microsc.* **192**, 217–226 (1998).
15. J. Bewersdorf, R. Pick, and S. W. Hell, "Multifocal multiphoton microscopy," *Opt. Lett.* **23**, 655–657 (1998).
16. S. W. Hell and V. Andersen, "Space-multiplexed multifocal nonlinear microscopy," *J. Microsc.* **202**, 457–463 (2001).
17. K. Fujita, O. Nakamura, T. Kaneko, S. Kawata, M. Oyama, and T. Takamatsu, "Real-time imaging of two-photon-induced fluorescence with a microlens-array scanner and a regenerative amplifier," *J. Microsc.* **194**, 528–531 (1999).
18. L. Sacconi, E. Froner, R. Antolini, M. R. Taghizadeh, A. Choudhury, and F. S. Pavone, "Multiphoton multifocal microscopy exploiting a diffractive optical element," *Opt. Lett.* **28**, 1918–1920 (2003).
19. M. Kobayashi, K. Fujita, T. Kaneko, T. Takamatsu, O. Nakamura, and S. Kawata, "Second-harmonic-generation microscope with a microlens array scanner," *Opt. Lett.* **27**, 1324–1326 (2002).

20. J.-X. Cheng and X. S. Xie, "Green's function formulation for third-harmonic generation microscopy," *J. Opt. Soc. Am. B* **19**, 1604–1609 (2002).
21. R. Boyd, *Nonlinear Optics* (Academic, New York, 1992).
22. V. V. Yakovlev and S. V. Govorkov, "Diagnostics of a surface layer disordering using optical third harmonic generation of a circular polarized light," *Appl. Phys. Lett.* **79**, 4136–4138 (2001).
23. D. Oron, E. Tal, and Y. Silberberg, "Depth-resolved multiphoton polarization microscopy by third-harmonic generation," *Opt. Lett.* **28**, 2315–2317 (2003).
24. D. Oron, D. Yelin, E. Tal, S. Raz, R. Fachima, and Y. Silberberg, "Depth-resolved structural imaging by third-harmonic generation microscopy," *J. Struct. Biol.* **147**, 3–11 (2004).
25. E. Beniash, J. Aizenberg, L. Addadi, and S. Weiner, "Amorphous calcium carbonate transforms into calcite during sea urchin larval spicule growth," *Proc. R. Soc. London, Ser. B* **264**, 461–465 (1997).
26. D. J. Ripin, C. Chudoba, J. T. Gopinath, J. G. Fujimoto, E. P. Ippen, U. Morgner, F. X. Kartner, V. Scheuer, G. Angelow, and T. Tschudi, "Generation of 20-fs pulses by a prismless  $\text{Cr}^{4+}$ :YAG laser," *Opt. Lett.* **27**, 61–63 (2002).
27. D. Yelin, D. Oron, E. Korokotian, M. Segal, and Y. Silberberg, "Third-harmonic microscopy with a titanium-sapphire laser," *Appl. Phys. B* **74**, s97–s101 (2002).